

STATIC AND DYNAMIC CHARACTERISTICS OF FINITE EXPONENTIAL FILM-SHAPED  
SLIDER BEARINGS LUBRICATED WITH NEWTONIAN FLUID

S. B. PATIL<sup>1\*</sup>, SIDDANGOUDA A<sup>2</sup> AND N. B. NADUVINAMANI<sup>3</sup>

<sup>1</sup>Department of Mathematics,  
Government First Grade College, Kalaburagi-585105, India.

<sup>2</sup>Department of Mathematics,  
Appa Institute of Engineering and Technology, Kalaburagi-585103, India.

<sup>3</sup>Department of Mathematics, Gulbarga University, Kalaburagi-585106, India.

(Received On: 16-11-15; Revised & Accepted On: 23-03-16)

---

ABSTRACT

*Analysis of dynamic characteristics plays an important role in designing hydrodynamic bearings. The analysis of dynamic characteristics for a finite slider bearing with exponential film profile is presented by taking into account the bearing squeezing action. The detailed analysis is presented for exponential film-shaped finite slider bearings by using perturbation technique. Two types of Reynolds equations pertaining to steady performance and the dynamic characteristics are obtained. The closed form solution of these equations is obtained by Numerical methods. Increasing values of aspect ratio (width-to-length ratio) enhances the pressure performance. Comparing with those of plane slider bearing, the exponential shaped slider bearing provides the higher values of load carrying capacity, stiffness coefficient and damping coefficient.*

**Keywords:** Dynamic characteristics, finite bearings, sliders, exponential film shape.

---

1. INTRODUCTION

Slider bearings are designed mainly to support the axial component of the load or thrust in a rotating shaft which passes through the casing of a perimeter. Analysis of the steady-state performance and dynamic characteristics of bearings taking into account the geometry and different operating conditions is important. The study of slider bearings with various film shapes lubricated with Newtonian fluids has been investigated by Hamrock [1], Pinkus and Sternlicht [2] and Cameron [3]. Bearing characteristics have been analyzed by considering different film shapes. Advanced analysis is presented by considering different operation conditions, such as the viscosity variation across the film [4], the inertia force effects [5-7], the turbulent flows [8-9], the temperature variation of fluid film [2], the thermal effects [10-13]. All these studies focus upon the performance of slider bearing operating under the steady state situation in which the effects of dynamic squeezing motion are neglected. It is known fact that the steady-state performance provides a basic reference in designing bearings. In order to avoid runner-pad contact and for predicting stability behavior of the bearing, a study of dynamic characteristics shows more important. An understanding of dynamic stiffness and damping behaviors is helpful in designing the bearing because the slider-bearing surfaces operate mainly upon the wedge-action principle. Lin et al [14] have analyzed the dynamic characteristics of wide slider bearings with an exponential film profile. To provide more information for the bearing designing, we are motivated to investigate the dynamic characteristics of the finite slider bearings with an exponential film profile.

On the basis of the thin film lubrication theory, this study is mainly concerned with the dynamic characteristics of finite slider bearings with an exponential film shape including the effects of squeezing action. The dynamic Reynolds-type equation, both of the steady-state Reynolds equation and the perturbed-type Reynolds equation are derived by applying a small perturbation technique. The steady-state performance and the dynamic characteristics of the bearings at different profile parameters and aspect ratio are then evaluated. Comparing with those of plane sliders, characteristics of bearings in terms of the steady load carrying capacity, dynamic stiffness and damping coefficient performance is better in case of exponential film profile.

---

**Corresponding Author: S. B. Patil<sup>1\*</sup>, <sup>1</sup>Department of Mathematics,  
Government First Grade College, Kalaburagi-585105, India.**

## 2. MATHEMATICAL FORMULATION OF THE PROBLEM

The physical geometry of the problem under consideration is shown in the Fig.1. It consists of an exponential-film slider bearing of length  $L$  and width  $B$  with sliding velocity  $U$  including the effect of squeezing action  $\frac{\partial h}{\partial t}$ ,  $h_1(t)$  is the inlet film thickness and outlet film thickness is  $h_0(t)$ . It is assumed that, the lubricant in the film region is Newtonian fluid. Newton's equations of motion are given by

$$\frac{\partial^2 u}{\partial z^2} = \frac{1}{\mu} \frac{\partial p}{\partial x}, \quad (1)$$

$$\frac{\partial^2 v}{\partial z^2} = \frac{1}{\mu} \frac{\partial p}{\partial y}, \quad (2)$$

$$\frac{\partial p}{\partial z} = 0, \quad (3)$$

$$\frac{\partial u}{\partial x} + \frac{\partial v}{\partial y} + \frac{\partial w}{\partial z} = 0, \quad (4)$$

where  $u$ ,  $v$  and  $w$  are the velocity components of the lubricant in the  $x$ ,  $y$  and  $z$  direction respectively. The relevant boundary conditions for the velocity components are

$$u = U, v = 0, w = 0 \quad \text{at } z = 0, \quad (5)$$

$$u = 0, v = 0, w = \frac{dH}{dt} \quad \text{at } y = H, \quad (6)$$

The solution of equations (1) and (2) subject to the boundary conditions (5) and (6) is obtained as

$$u = U - \frac{U}{H} z - \frac{1}{2\mu} \frac{\partial p}{\partial x} Hz + \frac{1}{2\mu} \frac{\partial p}{\partial x} z^2, \quad (7)$$

and 
$$v = -\frac{1}{2\mu} \frac{\partial p}{\partial y} Hz + \frac{1}{2\mu} \frac{\partial p}{\partial y} z^2, \quad (8)$$

Integrating the continuity equation (4) over the fluid film thickness and using the expressions (7) and (8) for  $u$  and  $v$  respectively and use the boundary conditions for  $w$  given in equations (5) and (6), the generalized Reynolds equation is obtained in the form

$$\frac{\partial}{\partial x} \left[ f(H) \frac{\partial p}{\partial x} \right] + \frac{\partial}{\partial y} \left[ f(H) \frac{\partial p}{\partial y} \right] = 6\mu U \frac{\partial H}{\partial x} + 1 \mu \frac{\partial H}{\partial t} \quad (9)$$

where  $f(H) = H^3$ .

### Exponential film shape slider bearing

To study the static and dynamic characteristics of exponential film-shaped slider bearing, the film thickness is separated into two parts: the minimum film thickness,  $h_m(t)$  and the exponential shaped slider profile function,  $h_e(x)$  i.e.

$$H(x,t) = H_m(t) H_e(x) = H_m(t) \exp \left[ -\frac{x}{L} \ln r \right] \quad \text{where } r \text{ denotes the inlet-outlet film ratio } r = \frac{H_1(t)}{H_0(t)}$$

$$= \left[ a + H_0(t) \right] / H_0(t), \quad \text{where } a \text{ is the shoulder height denoting the difference between the inlet and outlet height.}$$

Introducing the non-dimensional quantities

$$\bar{H} = \frac{H}{H_{m0}}, \quad \bar{H}_m = \frac{H_m}{H_{m0}}, \quad \bar{x} = \frac{x}{L}, \quad \bar{y} = \frac{y}{B},$$

$$\tau = \frac{Ut}{L}, \quad \lambda = \frac{a}{H_{m0}}, \quad \bar{P} = \frac{pH_{m0}^2}{\mu UL}, \quad \delta = \frac{B}{L}$$

into the dynamic Reynolds-type equation (7) we get

$$\frac{\partial}{\partial \bar{x}} \left[ \bar{f}(\bar{H}) \frac{\partial \bar{p}}{\partial \bar{x}} \right] + \frac{1}{\delta^2} \frac{\partial}{\partial \bar{y}} \left[ f(\bar{H}) \frac{\partial \bar{p}}{\partial \bar{y}} \right] = 1 - \mu \frac{\partial \bar{H}}{\partial \tau} + 6\mu \frac{\partial \bar{H}}{\partial \bar{x}}, \quad (10)$$

where  $\bar{f}(\bar{H}) = \bar{H}^3$ .

Since the linear dynamic characteristics can be obtained for the bearing under small disturbances about its steady-state, the inlet-outlet film ratio can be approximated by  $r = 1 + \lambda$  and the film thickness is then expressed as

$$\bar{H}(\bar{x}, \tau) = \bar{H}_m(\tau) \bar{H}_e(\bar{x}) = H_m(t) \exp \left[ -\frac{x}{L} \ln r \right].$$

### 3. SOLUTION OF THE PROBLEM

The steady and dynamic characteristics of the exponential film-shaped slider bearings are obtained by using the perturbations in  $H_m$ . The minimum film thickness and the local film pressure are assumed to be of the form

$$\bar{H}_m = 1 + \varepsilon e^{i\tau}, \quad \bar{P} = \bar{P}_0 + P_1 \varepsilon e^{i\tau} \quad (11)$$

where  $\varepsilon$  is the small perturbation amplitude and  $i = \sqrt{-1}$ . Substituting (11) into the non-dimensional dynamic Reynolds-type equation (10) and neglecting the higher order terms of  $\varepsilon$ , the two Reynolds-type equations corresponding to both steady-state pressure and the perturbed film pressure are obtained in the form

$$\frac{\partial}{\partial \bar{x}} \left[ \bar{f}_0 \frac{\partial \bar{P}_0}{\partial \bar{x}} \right] + \frac{1}{\delta^2} \bar{f}_0 \frac{\partial^2 \bar{P}_0}{\partial \bar{y}^2} = -6 \ln(1 + \lambda) \bar{H}_e(\bar{x}), \quad (12)$$

$$\frac{\partial}{\partial \bar{x}} \left[ \bar{f}_0 \frac{\partial \bar{P}_1}{\partial \bar{x}} + \bar{f}_1 \frac{\partial \bar{P}_0}{\partial \bar{x}} \right] + \frac{1}{\delta^2} \left[ \bar{f}_0 \frac{\partial^2 \bar{P}_1}{\partial \bar{y}^2} + \bar{f}_1 \frac{\partial^2 \bar{P}_0}{\partial \bar{y}^2} \right] = 6 \left[ 2i - \ln(1 + \lambda) \right] \bar{H}_e(\bar{x}) \quad (13)$$

where

$$\bar{f}_0 = \bar{H}_e^3(\bar{x}), \quad \bar{f}_1 = 3\bar{H}_e(\bar{x}) \quad (14)$$

The relevant boundary conditions for the steady state and perturbed film pressure are

$$\bar{P}_0 = 0 \quad \text{at } \bar{x} = 0, \quad \bar{x} = -1, \quad \bar{y} = 0, \quad \bar{y} = 1; \quad (15)$$

$$\bar{P}_1 = 0 \quad \text{at } \bar{x} = 0, \quad \bar{x} = -1, \quad \bar{y} = 0, \quad \bar{y} = 1. \quad (16)$$

The modified Reynolds equation will be solved numerically by using a finite difference scheme. The film domain under consideration is divided by the grid spacing as shown in Fig.2. In finite increment format, the terms in the Eqn. (12) and Eqn. (13) can be expressed as

$$\frac{\partial}{\partial \bar{x}} \left( \bar{f}_0 \frac{\partial \bar{P}_0}{\partial \bar{x}} \right) = \frac{1}{\Delta \bar{x}} \left[ \bar{f}_{0i+\frac{1}{2},j} \left( \frac{\bar{P}_{0i+1,j} - \bar{P}_{0i,j}}{\Delta \bar{x}} \right) - \bar{f}_{0i-\frac{1}{2},j} \left( \frac{\bar{P}_{0i,j} - \bar{P}_{0i-1,j}}{\Delta \bar{x}} \right) \right], \quad (17)$$

$$\bar{f}_0 \frac{\partial^2 \bar{P}_0}{\partial \bar{y}^2} = \frac{1}{(\Delta \bar{y})^2} \bar{f}_{0i,j} [\bar{P}_{0i,j+1} - 2\bar{P}_{0i,j} + \bar{P}_{0i,j-1}], \quad (18)$$

$$\begin{aligned} \frac{\partial}{\partial \bar{x}} \left[ \bar{f}_0 \frac{\partial \bar{P}_1}{\partial \bar{x}} + \bar{f}_1 \frac{\partial \bar{P}_0}{\partial \bar{x}} \right] &= \frac{1}{\Delta \bar{x}} \left[ \bar{f}_{0i+\frac{1}{2},j} \left( \frac{\bar{P}_{1i+1,j} - \bar{P}_{1i,j}}{\Delta \bar{x}} \right) - \bar{f}_{0i-\frac{1}{2},j} \left( \frac{\bar{P}_{1i,j} - \bar{P}_{1i-1,j}}{\Delta \bar{x}} \right) \right] \\ &+ \frac{1}{\Delta \bar{x}} \left[ \bar{f}_{1i+\frac{1}{2},j} \left( \frac{\bar{P}_{0i+1,j} - \bar{P}_{0i,j}}{\Delta \bar{x}} \right) - \bar{f}_{1i-\frac{1}{2},j} \left( \frac{\bar{P}_{0i,j} - \bar{P}_{0i-1,j}}{\Delta \bar{x}} \right) \right] \end{aligned} \quad (19)$$

and

$$\bar{f}_0 \frac{\partial^2 \bar{P}_1}{\partial \bar{y}^2} + \bar{f}_1 \frac{\partial^2 \bar{P}_0}{\partial \bar{y}^2} = \frac{1}{(\Delta \bar{y})^2} \bar{f}_{0i,j} [\bar{P}_{1i,j+1} - 2\bar{P}_{1i,j} + \bar{P}_{1i,j-1}] + \frac{1}{(\Delta \bar{y})^2} \bar{f}_{1i,j} [\bar{P}_{0i,j+1} - 2\bar{P}_{0i,j} + \bar{P}_{0i,j-1}] \quad (20)$$

After the substitution for the above finite difference forms, the steady-state and perturbed Reynolds equations (12) and (13) leads to

$$\bar{P}_{0i,j} = c_1 \bar{P}_{0i+1,j} + c_2 \bar{P}_{0i-1,j} + c_3 \bar{P}_{0i,j+1} + c_4 \bar{P}_{0i,j-1} + c_5, \quad (21)$$

$$\begin{aligned} \bar{P}_{1rp i,j} = & c_1 \bar{P}_{1rp i+1,j} + c_2 \bar{P}_{1rp i-1,j} + c_3 \bar{P}_{1rp i,j+1} + c_4 \bar{P}_{1rp i,j-1} \\ & + c_6 \bar{P}_{0i+1,j} + c_7 \bar{P}_{0i-1,j} + c_8 \bar{P}_{0i,j+1} + c_9 \bar{P}_{0i,j-1} + c_1 \bar{P}_{0i,j} + C_1, \end{aligned} \quad (22)$$

$$\bar{P}_{lip i,j} = c_1 \bar{P}_{lip i+1,j} + c_2 \bar{P}_{lip i-1,j} + c_3 \bar{P}_{lip i,j+1} + c_4 \bar{P}_{lip i,j-1} + c_1 \quad (23)$$

where the perturbed film pressure has been expressed in terms of real and imaginary parts

$$\bar{p}_1 = \bar{p}_{1rp} + i \bar{p}_{lip}. \quad (24)$$

The coefficients  $c_0$  to  $c_{12}$  are defined as

$$\begin{aligned} c_0 &= \delta^2 b^2 \left( \bar{f}_{0i+\frac{1}{2},j} + \bar{f}_{0i-\frac{1}{2},j} \right) + 2\bar{f}_{0i,j}, \\ c_1 &= \delta^2 b^2 \bar{f}_{0i+\frac{1}{2},j} / c_0, \\ c_2 &= \delta^2 b^2 \bar{f}_{0i-\frac{1}{2},j} / c_0, \\ c_3 &= c_4 = \bar{f}_{0i,j} / c_0, \\ c_5 &= 6\delta^2 \ln(1+\lambda) (\Delta\bar{y})^2 \bar{H}_e(\bar{x}) / c_0, \\ c_6 &= \delta^2 b^2 \bar{f}_{1i+\frac{1}{2},j} / c_0, \\ c_7 &= \delta^2 b^2 \bar{f}_{1i-\frac{1}{2},j} / c_0, \\ c_8 &= c_9 = \bar{f}_{1i,j} / c_0, \\ c_{10} &= \left[ \delta^2 b^2 \left( \bar{f}_{1i+\frac{1}{2},j} + \bar{f}_{1i-\frac{1}{2},j} \right) + 2\bar{f}_{1i,j} \right] / c_0, \\ c_{11} &= 6\delta^2 \ln(1+\lambda) (\Delta\bar{y})^2 \bar{H}_e(\bar{x}) / c_0, \\ c_{12} &= -12\delta^2 (\Delta\bar{y})^2 \bar{H}_e(\bar{x}) / c_0, \text{ and } b = \Delta\bar{y} / \Delta\bar{x}. \end{aligned}$$

The steady-state film pressure and the perturbed film pressure are then calculated by using numerical method with grid spacing of  $\Delta\bar{x} = \Delta\bar{y} = 0.05$ . The steady-state load carrying capacity,  $W_s$  and perturbed film force,  $W_d$  are evaluated by integrating the steady-state film pressure and perturbed film pressure respectively over the film region.

$$W_s = \frac{\mu UL^2 B}{H_{m0}^2} \int_{x=0}^{x=-L} \int_{y=0}^{y=B} P_0 dx dy, \quad (25)$$

$$W_d = \frac{\mu UL^2 B}{H_{m0}^2} \int_{x=0}^{x=-L} \int_{y=0}^{y=B} P_1 dx dy, \quad (26)$$

which in non-dimensional form

$$\begin{aligned} \bar{W}_s &= \frac{W_s H_{m0}^2}{\mu UL^2 B} = \int_{\bar{x}=0}^{\bar{x}=-1} \int_{\bar{y}=0}^{\bar{y}=1} \bar{P}_0 d\bar{x} d\bar{y}, \\ &\approx \sum_{i=0}^M \sum_{j=0}^N \bar{P}_{0i,j} \Delta\bar{x} \Delta\bar{y} \end{aligned} \quad (27)$$

$$\bar{W}_d = \frac{W_d H_{m0}^2}{\mu U L^2 B} = \int_{\bar{x}=0}^{\bar{x}=-1} \int_{\bar{y}=0}^{\bar{y}=1} \bar{P}_1 d\bar{x} d\bar{z} \quad (28)$$

$$\approx \sum_{i=0}^M \sum_{j=0}^N \bar{P}_{1i,j} \Delta\bar{x} \Delta\bar{y}$$

where  $M+1$  and  $N+1$  are the number of grid points in the  $x$  and  $z$  directions respectively.

From the linear theory, the resulting dynamic film force can be expressed in terms of linearized spring and damping coefficients.

$$W_d \varepsilon e^{i\tau} = -S_d H_{m0} \varepsilon e^{i\tau} - C_d \frac{d}{dt} (H_{m0} \varepsilon e^{i\tau}), \quad (29)$$

which in non-dimensional form

$$\bar{W}_d = -\bar{S}_d - i \bar{C}_d, \quad (30)$$

where

$$\bar{S}_d = \frac{S_d H_{m0}^3}{\mu U L^2 B} \quad \text{and} \quad \bar{C}_d = \frac{C_d H_{m0}^3}{\mu L^3 B}$$

The non-dimensional dynamic stiffness coefficient,  $\bar{S}_d$  and dynamic damping coefficient,  $\bar{C}_d$  are obtained by equating the real and imaginary parts of  $\bar{W}_d$  respectively as

$$\bar{S}_d = -\text{Re}(\bar{W}_d) \approx -\sum_{i=0}^M \sum_{j=0}^N (\bar{P}_{1rp})_{i,j} \Delta\bar{x} \Delta\bar{y}. \quad (31)$$

$$\bar{C}_d = -\text{Im}(\bar{W}_d) \approx -\sum_{i=0}^M \sum_{j=0}^N (\bar{P}_{1ip})_{i,j} \Delta\bar{x} \Delta\bar{y}. \quad (32)$$

#### 4. RESULTS AND DISCUSSION

Considering the transient squeezing-action effects, the dynamic characteristics of an exponential film shaped finite slider bearings lubricated with Newtonian fluid are investigated. Both of the steady-state performance and the dynamic characteristics are analyzed by applying a small perturbation technique. In this paper we have compared plane slider bearing with an exponential shaped slider bearing for steady state film pressure, steady load carrying capacity, stiffness coefficient and damping coefficient. Figure 3 shows the variation of steady state film pressure,  $\bar{P}_0$  with  $x$ -axis for different values of aspect ratio,  $\delta$ . It is observed that increasing values of aspect ratio,  $\delta$  increases the state film pressure. Figures 4 and 5 shows the variation of dimensionless steady load-carrying capacity,  $\bar{W}_s$  with profile parameter,  $\lambda$  and aspect ratio,  $\delta$  respectively. The dotted curve shows the results for finite plane slider bearing obtained by Naduvinamani et al [14]. The solid curve presents the steady load-carrying capacity for the present study. Comparing with those of the inclined plane slider, the exponential shaped slider provides a higher load-carrying capacity for larger values of the profile parameter.

Figures 6 and 7 shows the variation of dimensionless dynamic stiffness coefficient,  $\bar{S}_d$  with the profile parameter,  $\lambda$  and aspect ratio,  $\delta$  respectively. It is observed for the inclined plane slider that the maximum stiffness coefficient lies within the range of small values of the profile parameter. But the maximum stiffness shifts to the position of a larger  $\lambda$  for the exponential shaped bearing. Comparing with the inclined-plane slider, the slider with an exponential shaped film results in a significantly increased stiffness for larger values of the profile parameter,  $\lambda$  and aspect ratio,  $\delta$ .

The variation of non-dimensional damping coefficient,  $\bar{C}_d$  with the profile parameter  $\lambda$  and the aspect ratio,  $\delta$  is illustrated in figures 8 and 9. For both types of bearings, increasing value of  $\lambda$  yields a decreasing damping coefficient. Comparing with those of the inclined plane slider, the exponential shaped slider provides a higher damping coefficient especially for larger values of the profile parameter  $\lambda$ . Comparing with those of the inclined plane slider, the exponential shaped slider provides higher damping coefficient for increasing values of aspect ratio,  $\delta$ .

## 5. CONCLUSIONS

In this paper, on the basis of the thin-film lubrication theory, a study of dynamic characteristics for a exponential shaped finite slider bearing considering the squeezing action is presented. Both the steady-state performance and the dynamic characteristics are evaluated by applying a small perturbation technique to the dynamic Reynolds-type equation.

Both of the steady-state performance and the dynamic characteristics are significantly affected by both the profile parameter,  $\lambda$  and aspect ratio,  $\delta$ . Comparing with those of the inclined plane slider by Naduvinamani et al [15], the exponential shaped slider provides higher load-carrying capacity and better dynamic stiffness and damping coefficient for increasing values of profile parameter,  $\lambda$  and aspect ratio,  $\delta$ . This analysis provides the useful information for engineers in designing and application of bearing systems.

## REFERENCES

1. B. J. Hamrock: 'Fundamentals of fluids film lubrication', 1994, New York, McGraw-Hill.
2. O. Pinkus and B. Sternlicht: 'Theory of hydrodynamic lubrication'', 1961, New York, McGraw-hill.
3. A. Cameron: 'The principles of lubrication', 1966, London, Longmans Green and Co Ltd.
4. Qvale E. B. and Witshire F. R., "The performance of Hydrodynamic Lubricating Films with viscosity variations perpendicular to the Direction of Motion" ASME J. Lubr. Technol. 94, 1972, 44-48
5. Launder B. E. and Leschziner M.L. "Flow in Finite-width, Thrust Bearings including Inertia Effects", ASME J. Lubr. Technol, 100, 1987, 330-338
6. Rodkiewicz C.M. and Anwar M.I. "Inertia and convective Effect in Hydrodynamic Lubrication of a Slider Bearing", ASME J. Lubr. Technol. 93, 1971, 313-315
7. Synder W. T. "The Nonlinear Hydrodynamic Slider Bearing", ASME J. Basic Engr 85, 1963, 429-434
8. King K.F. and Taylor C.M. "An estimation of the Effect Fluid Inertia on the performance of the plane Inclined Slider Thrust Bearing with particular regard to Turbulent Lubrication" ASME J. Lubr. Technol 99 1997, 129-135
9. Taylor CM and Dowson D. "Turbulent Lubrication Theory-Application to Design". ASME J. Lubr. Technol. 96 1974 36-46
10. Chowdhury SJ and Ahmadi G. "Thermodynamic Analysis of Wide Thrust Bearings operating in Laminar Inertial Flow Regimes" ASME J Lubr. Technol, 19 1986 281-288
11. Rodkiewicz C.M., Hinds JC and Dayson C. "Inertia, Convective and Dissipation Effects in the Thermally Boosted oil Lubricated Slider Thrust Bearing" ASME J. Lubr Technol 97, 1975, 121-129
12. Safer Z. S. "Thermal and Inertia Effects in Turbulent Flow Thrust Bearing" Proc I Mech E. 22, 1980, 43-45
13. Talmage G and Carpino M. "A Pseudospectral-Finite Difference Analysis of an infinitely wide slider Bearings with Thermal and Inertia Effects" STLE Tribol Transact 40 1997 251-255
14. Jaw-Ren Lin and Chi-Ren Hung "Analysis of dynamic characteristics for wide slider bearings with an exponential film profile" Journal of Marine Science and Technology 12(3) 2004 217-221
15. N. B. Naduvinamani and G. B. Marali: *Proc. Instn Mech. Engrs, Part J, J. Engineering Tribology* 2007, 221, 82-829

## LIST OF SYMBOLS

$a$	difference between the inlet and outlet film thickness ( $= h_1(t) - h_0(t)$ )
$B$	bearing width
$C_d$	dynamic damping coefficient
$\bar{C}_d$	non-dimensional dynamic damping coefficient $\left( = \frac{C_d h_{m0}^3}{\mu L^3 B} \right)$
$h$	film thickness function (defined in Eqn (1))
$\bar{h}$	non-dimensional film thickness function $\left( = \frac{h}{h_{m0}} \right)$
$h_m$	minimum film thickness function
$h_{m0}$	minimum film thickness under steady state
$h_e$	exponential profile function of the bearing

$\bar{h}_e$	non-dimensional exponential profile function $\left( = \frac{h_e}{h_{m0}} \right)$
$i$	$\sqrt{-1}$
$L$	bearing length
$l$	characteristic material length $\left( = \left( \frac{\gamma}{4\mu} \right)^{\frac{1}{2}} \right)$
$\bar{l}$	non-dimensional characteristic material length $\left( = \frac{l}{h_{m0}} \right)$
$N$	coupling number $\left( = \left( \frac{\chi}{\chi + 2\mu} \right)^{\frac{1}{2}} \right)$
$p_0$	steady film pressure
$\bar{P}_0$	non-dimensional steady film pressure $\left( = \frac{p_0 h_{m0}^2}{\mu UL} \right)$
$p_1$	perturbed film pressure
$\bar{P}_1$	non-dimensional perturbed film pressure $\left( = \frac{p_1 h_{m0}^2}{\mu UL} \right)$
$S_d$	dynamic stiffness coefficient
$\bar{S}_d$	non-dimensional dynamic stiffness coefficient $\left( = \frac{S_d h_{m0}^3}{\mu UL^2 B} \right)$
$t$	time
$\tau$	non-dimensional response time
$U$	sliding velocity
$W_d$	perturbed film force
$\bar{W}_d$	non-dimensional perturbed film force $\left( = \frac{W_d h_{m0}^2}{\mu UL^2 B} \right)$
$W_s$	steady load-carrying capacity
$\bar{W}_s$	non-dimensional steady load-carrying capacity $\left( = \frac{W_s h_{m0}^2}{\mu UL^2 B} \right)$
$x, y, z$	cartesian rectangular coordinates
$\delta$	aspect ratio of the bearing $(=B/L)$
$\varepsilon$	small amplitude of oscillation
$\gamma, \chi$	viscosity coefficients for micropolar fluids
$\lambda$	profile parameter of the bearing $\left( = \frac{a}{h_{m0}} \right)$
$\mu$	classical viscosity coefficient

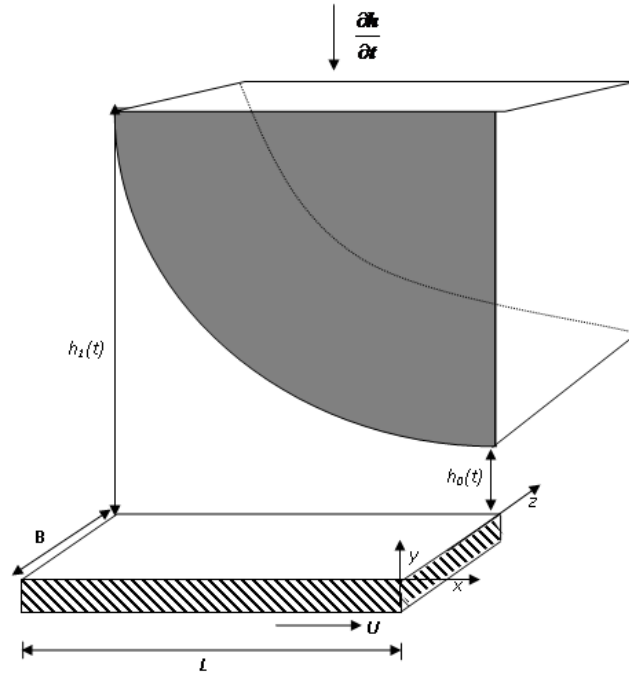


Fig.1: Physical geometry of an exponential – film slider bearing

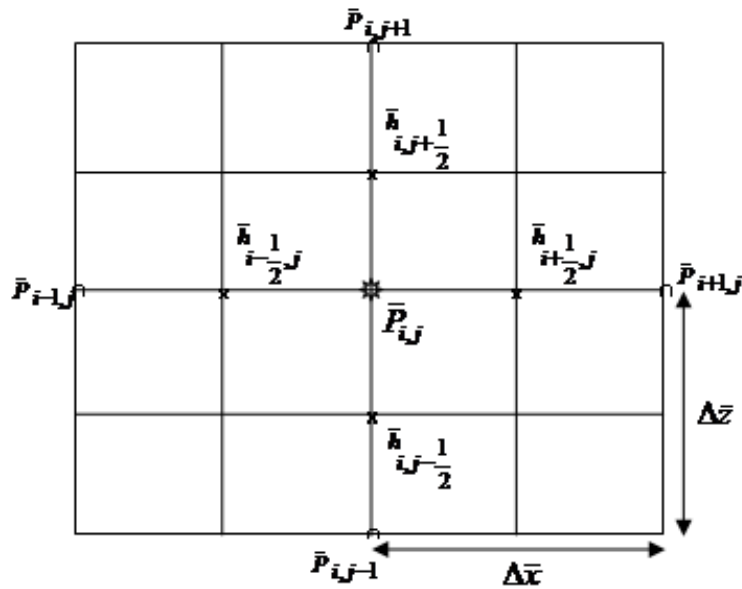
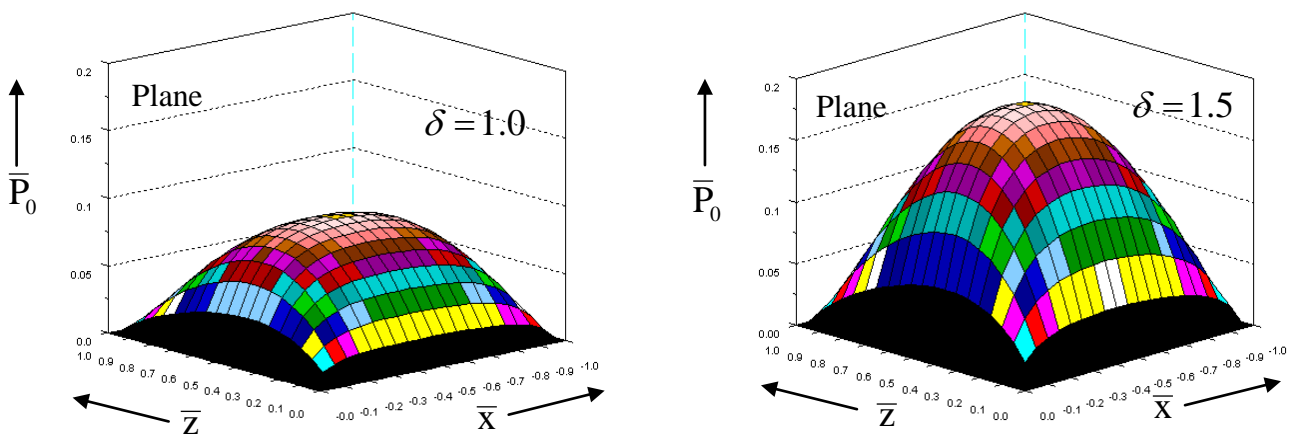


Fig.2: Grid point notation for film domain





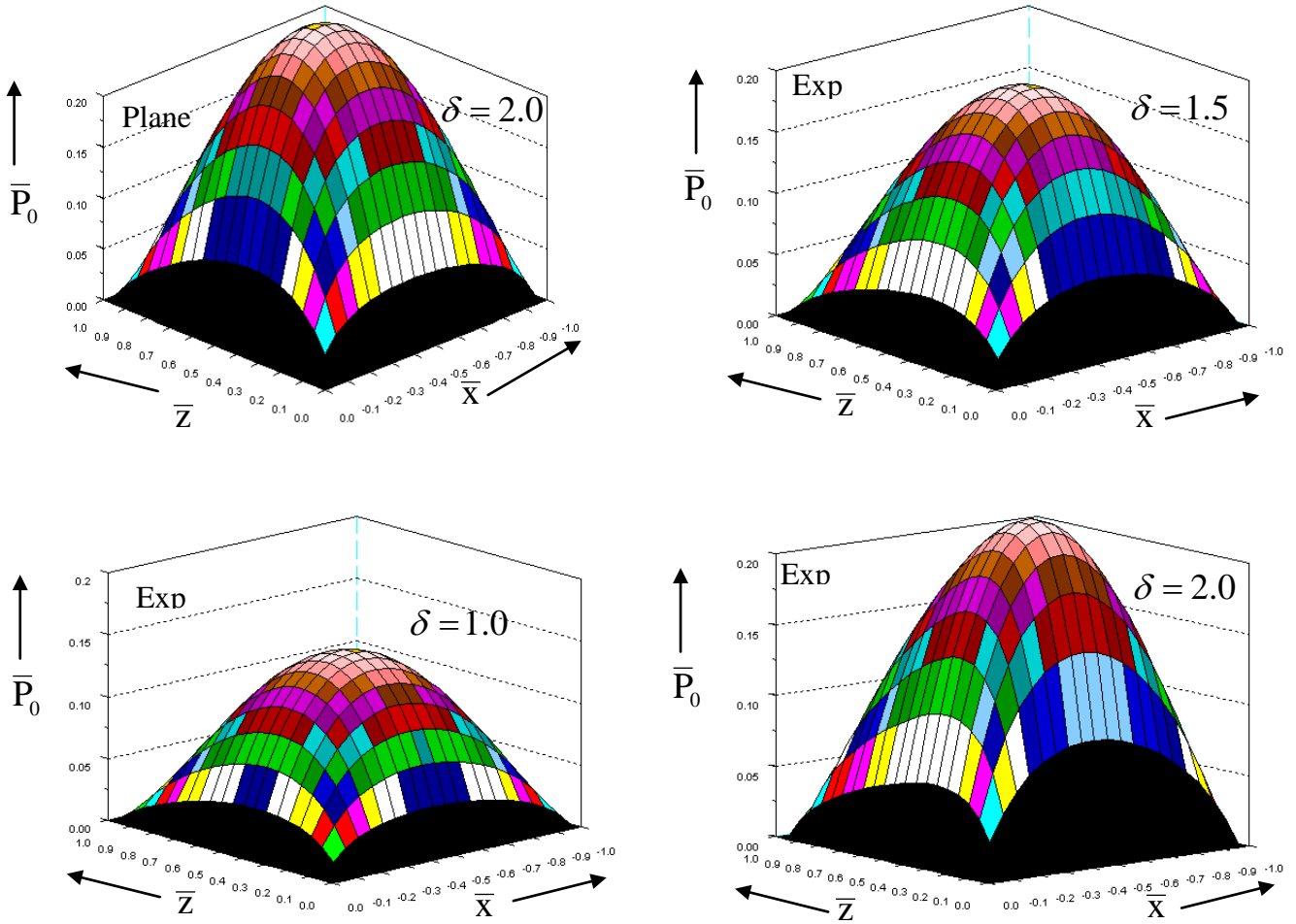


Fig.3: Non-dimensional steady-state film pressure  $\bar{P}_0$  for different values of aspect ratio  $\delta$  with  $\lambda=0.75$

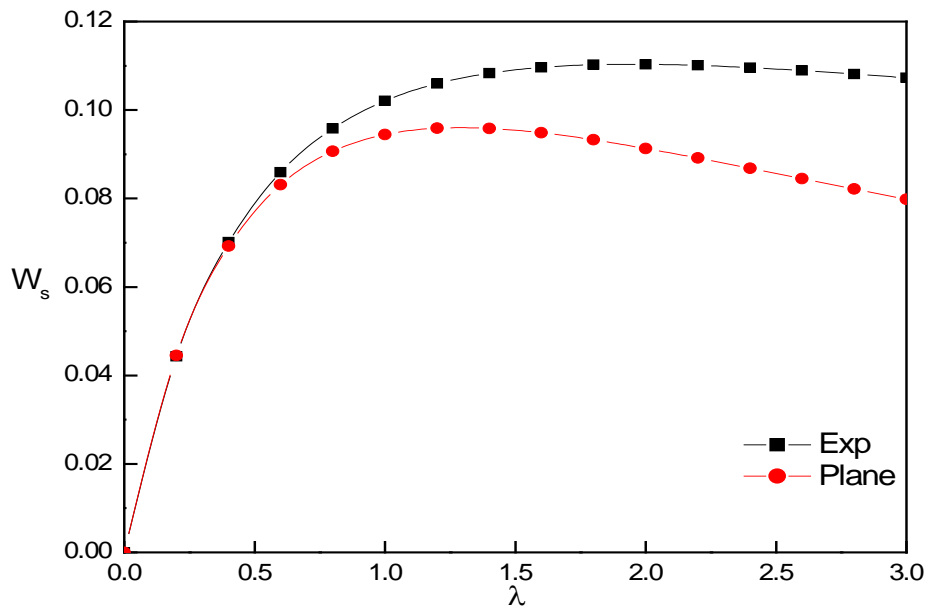


Fig.4 Variation of non-dimensional steady load carrying capacity  $W_s$  with profile parameter  $\lambda$  for  $\delta = 1.5$

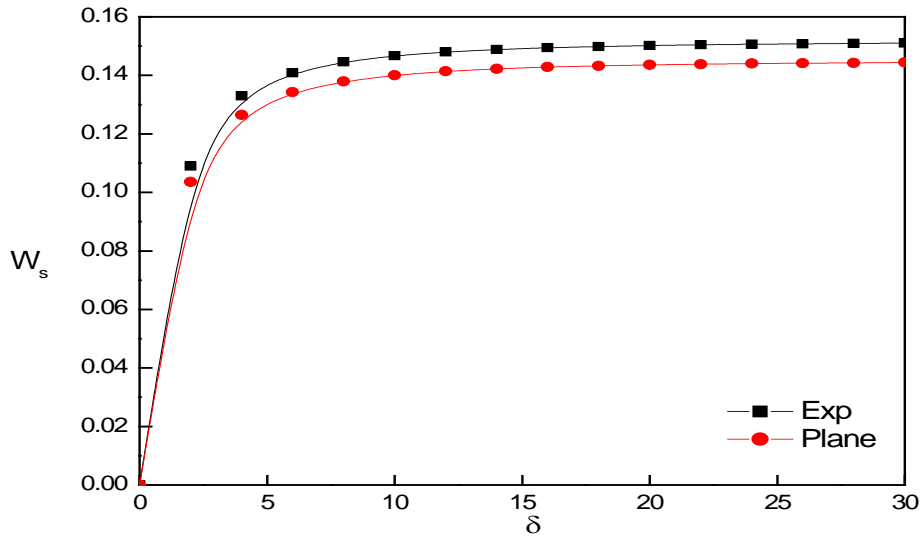


Fig.5 Variation of non-dimensional steady load carrying capacity  $W_s$  with aspect ratio  $\delta$  for  $\lambda=0.75$

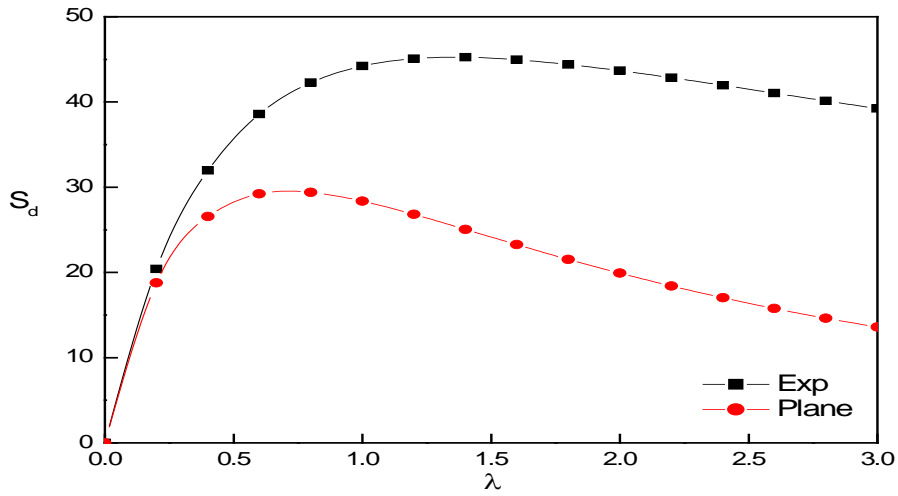


Fig.6 Variation of non-dimensional dynamic stiffness coefficient  $S_d$  with profile parameter  $\lambda$  for  $\delta=1.5$

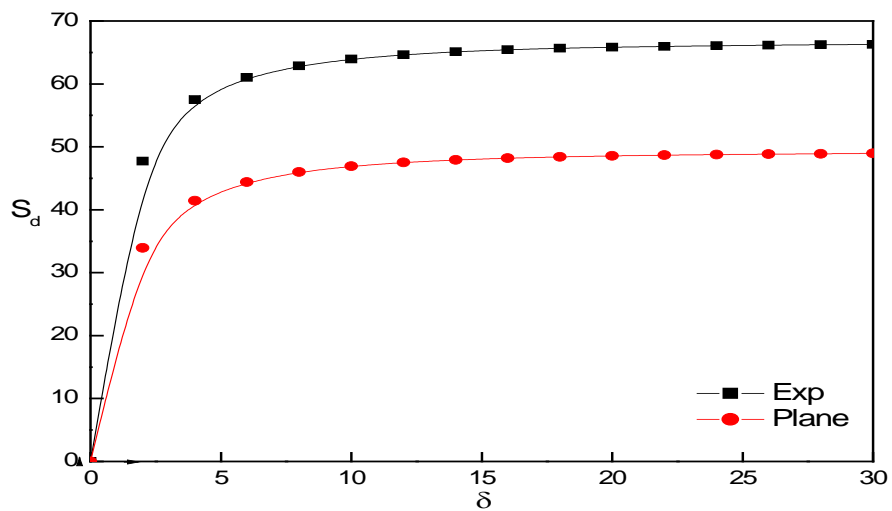


Fig.7 Variation of non-dimensional dynamic stiffness coefficient  $S_d$  with aspect ratio  $\delta$  for  $\lambda=0.75$

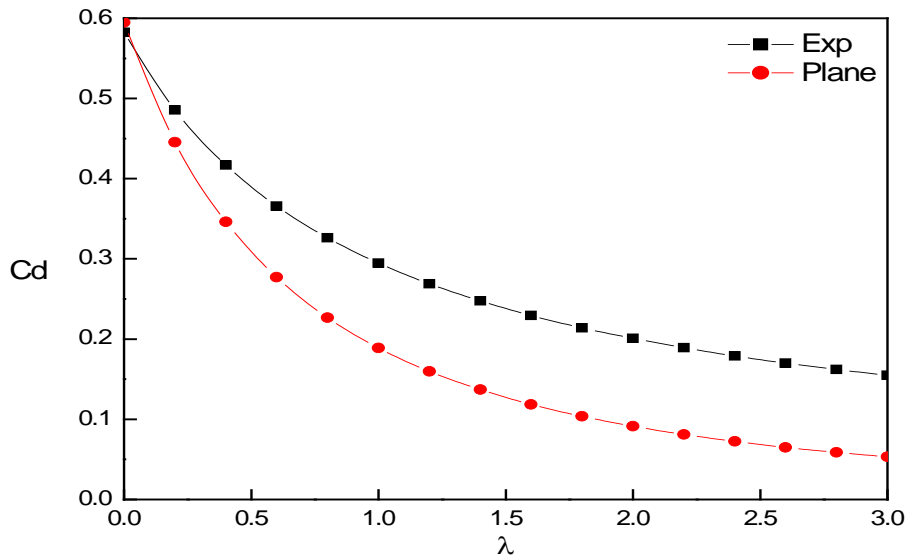


Fig.8 Variation of non-dimensional dynamic damping coefficient  $C_d$  with profile parameter  $\lambda$  for  $\delta=1.5$

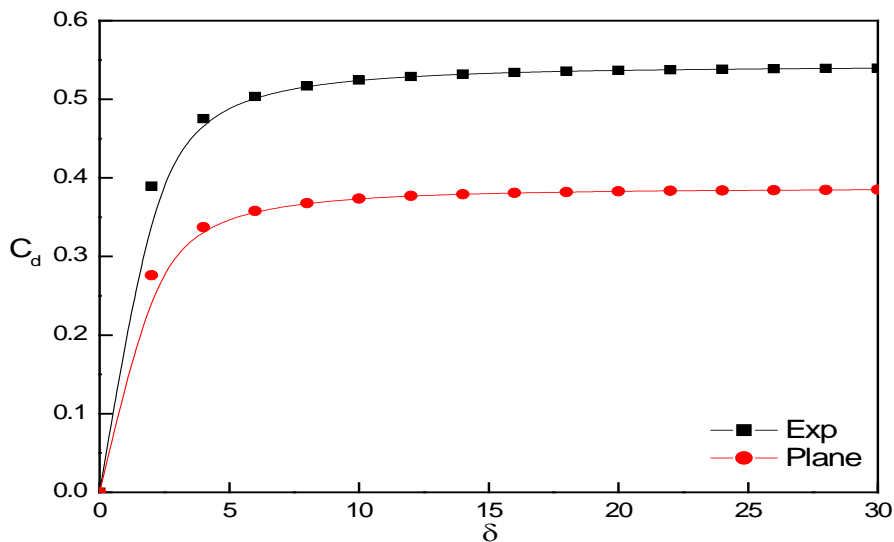


Fig.9 Variation of non-dimensional dynamic damping coefficient  $C_d$  with aspect ratio  $\delta$  for  $\lambda=0.75$

Source of support: Nil, Conflict of interest: None Declared

[Copy right © 2016. This is an Open Access article distributed under the terms of the International Journal of Mathematical Archive (IJMA), which permits unrestricted use, distribution, and reproduction in any medium, provided the original work is properly cited.]